Tri- and tetra-substituted derivatives of [Fe2(CO)6(μ-dithiolate)] as novel dinuclear platforms related to the H-cluster of [FeFe]H2ases

Francesca Realini, Catherine Elleouet, François Y. Pétillon, Philippe P. Schollhammer

EurJIC
European Journal of Inorganic Chemistry

Research Article
doi.org/10.1002/ejic.202200133

Chemistry Europe
European Chemical Societies Publishing

www.eurjic.org

Special Collection

Tri- and Tetra-Substituted Derivatives of $[Fe_2(CO)_6(\mu\text{-dithiolate})]$ as Novel Dinuclear Platforms Related to the H-Cluster of $[FeFe]H_2$ases

Francesca Realini,[a] Catherine Elleouet,*[a] François Y. Pétillon,[a] and Philippe Schollhammer*[a]

Dedicated to Professor Rinaldo Poli on the occasion of his 65th birthday

Novel carbonyl dithiolato diiron complexes $[Fe_2(CO)_{6-x}L_x(\mu\text{-dithiolate})]$ (x = 3, 4), related to the active site of [FeFe]-hydrogenases, have been synthesized by photolysis of hexacarbonyl species $[Fe_2(CO)_6(\mu\text{-dithiolate})]$ (dithiolate = $\{S_2(CH_2)_3\}$ (pdt), $\{SCH_2\}_2NR$ with R = ^{i}Pr (adt^{i-Pr}) or Bn (adt^{Bn})). The new compounds were characterized by structural and spectroscopic methods. Variable-temperature (VT) NMR experiments revealed their fluxionality in solution depending on terminal ligands exchanges and dithiolate bridge motions. Preliminary results on their protonation giving hydride species and their electrochemical properties are reported.

Introduction

The active site of [FeFe] hydrogenases, the H-cluster, is an outstanding example of a natural chemical engineering device that associates bimetallic and metal-ligand cooperativities through the presence of redox and proton relay for controlling its activity at the molecular level.[1,2] It can be considered as a highly sophisticated archetype for bimetallic activation. During the last decades, the chemistry of synthetic diiron species have been developed in order to reproduce the bidirectional behaviour of this enzyme towards H^+/H_2 conversion, and to demonstrate that diiron systems could be inserted in applicative device for the production of H_2.[3–5] Several works still continue to contribute to solve the question of the redox/protonated stages of catalytically active intermediates involved into the intricated mechanism of functioning of the H-cluster.[6–8] The questions of controlling proton and electron circulation as well as how generating specific redox/protic conformations affording a free coordination site and active hydride species at bimetallic moieties are at the heart of several studies and remain opened for chemists. Interestingly, Zampella *et coll.* examined recently, by density functional theory, the possibility to obtain with polysubstituted diiron complexes $[Fe_2(CO)_2L_4(\mu\text{-dithiolate})]$ bridging hydride species more reactive than their kinetic terminal hydride isomers while the opposite is thermodynamically expected and generally observed.[9] The behaviours of these diiron models depend a lot on fine electronic/steric combinations of the dithiolate bridge and terminal ligands.[3,10] The replacement of CO ligands by various better donating ligands in hexacarbonyl diiron Fe(I)Fe(I) precursors $[Fe_2(CO)_6(\mu\text{-dithiolate})]$ is a straight way for modifying the electronic/steric properties of the diiron core but such a strategy mainly depends on the reactional conditions (thermolysis, photolysis, use of reagent (Me_3NO)) which induces the replacement of one or more carbonyl groups. It is worth noting that the chemistry of substituted diiron species $[Fe_2(CO)_{6-x}L_x(\mu\text{-dithiolate})]$ with x > 3 has been not extensively studied by using different monodentate or polydentate ligands compared to that of mono and disubstituted derivatives (x = 1, 2) despite the fact that important insights have been obtained with bis-chelate derivatives.[3] For these reasons, we have started to prepare a series of tri- and tetra-substituted derivatives $[Fe_2(CO)_{6-x}L_x(\mu\text{-dithiolate})]$ with $x \geq 3$. We report in this short communication our preliminary results on the preparation, characterization, and behaviour of novel relatively stable tri- and tetra-substituted diiron species obtained by using the monodentate phosphite $P(OMe)_3$.

Results and Discussion

The formation of mono- and di-substituted diiron dithiolate complexes $[Fe_2(CO)_{6-x}L_x(\mu\text{-dithiolate})]$ (x = 1, 2) have been reported with the monodentate phosphite $P(OMe)_3$ (L).[11] To the best of our knowledge the related tri- and tetra-substituted derivatives are unknown until now. Only the photolysis of a bis-

[a] F. Realini, Ass. Prof. Dr. C. Elleouet, Prof. Dr. em. F. Y. Pétillon, Prof. Dr. P. Schollhammer
UMR CNRS 6521 Chimie,
Electrochimie Moléculaires et Chimie Analytique,
Université de Bretagne Occidentale,
UFR Sciences et Techniques
6 Avenue Victor le Gorgeu, CS 93837, 29238 Brest-Cedex 3, France
E-mail: catherine.elleouet@univ-brest.fr
philippe.schollhammer@univ-brest.fr

Supporting information for this article is available on the WWW under https://doi.org/10.1002/ejic.202200133

Part of the "celebratory collection for Rinaldo Poli".

Research Article
doi.org/10.1002/ejic.202200133

Chemistry Europe
European Chemical Societies Publishing

thiolate complex, $[Fe_2(CO)_6(\mu\text{-}S\text{-}^tBu)_2]$, affording a compound presumed to be $[Fe_2(CO)_3\{P(OMe)_3\}_3(\mu\text{-}S\text{-}^tBu)_2]$, was reported[11a] and a handful of tetra-substituted compounds containing PMe_3 have been described in literature.[12] Photolytic route was used for preparing the series of tri- and tetra-substituted diiron dithiolato complexes from tetrahydrofuran solutions of hexacarbonyl diiron precursors $[Fe_2(CO)_6(\mu\text{-xdt})]$ (xdt = pdt (**1 a**), adt^{i-Pr} (**1 b**), and adt^{Bn} (**1 c**)) in the presence of an excess of $P(OMe)_3$ (Scheme 1). Thermolysis of **1 a–c** affords only mono and disubstituted species. The substituted derivatives were separated and purified by chromatography on a silica gel column, and characterized by spectroscopic methods (IR, NMR), and/or X-ray diffraction methods. All the complexes were obtained in low or moderate yields after purification. Complexes **2 c** and **3 a–b** crystallized by slow evaporation of n-pentane solutions either at room temperature (**3 a**) or at lower temperature (**3 b**, **2 c**). Their molecular structures were determined by X-ray analysis (Table S1 for crystallographic data and refinement parameters). The molecular structures of the tetra-substituted complexes **3 a–b** are very similar, presenting the phosphite ligands in a transoïd basal-apical arrangement at each iron atom (Figure 1). In the tri-substituted derivative **2 c** one $P(OMe)_3$ ligand is coordinated at one iron atom in apical position and the two others at the second iron centre in basal-apical disposition. In these dinuclear Fe^IFe^I complexes, the iron atoms have a square-pyramidal geometry, as confirmed by the values of the P–Fe-P, P–Fe-CO, P–Fe-S, S–Fe-S, and S–Fe-CO angles (Table 1). The crystallographic analysis indicates that **3 a–b** have similar structures than those of the related phosphine tetra-substituted compounds $[Fe_2(CO)_2(PMe_3)_4(\mu\text{-xdt})]$ (xdt = pdt, edt) (edt = $\{S_2(CH_2)_2\}$).[12c] The benzyl group in **2 c** is in equatorial position relatively to the six members metallacycle FeS_2C_2N. It is worthy to note that increasing the number of substitutions of CO ligands by better donor ones, such as $P(OMe)_3$, results clearly in a concomitant lengthening of the iron-iron bond distance in these complexes. For example, the Fe–Fe length of 2.5089(4) Å in the di-substituted compound $[Fe_2(CO)_4\{P(OMe)_3\}_2(\mu\text{-pdt})]$[11c] increases up to 2.5584(3) Å in the tri-substituted derivative **2 c**, and ~2.60 Å in the tetra-substituted complexes **3 a–b**. Such a feature has been attributed to higher partial occupancy of the LUMO, which is known to be anti-bonding with regard to the Fe–Fe bond.[13] The iron-iron lengths in these three compounds (**2 c** and **3 a–b**) accord with a Fe–Fe single bond of a complex having a 18 electron counting rule.

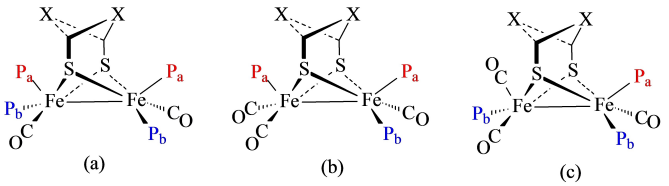

Scheme 2. Fluxional process operative in tri- and tetra-substituted derivatives (OMe substituents are omitted for clarity; a = apical, b = basal).

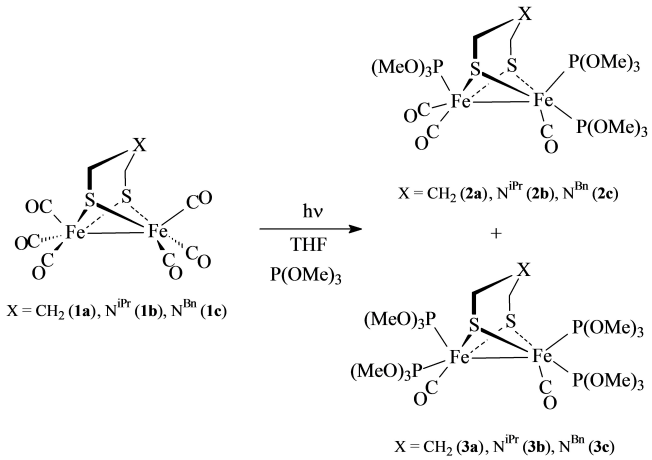

Scheme 1. Syntheses of tri-and tetra-substituted diiron dithiolate compounds.

Table 1. Selected distances and bond angles of complexes **2 c**, **3 a–b**.

		2 c	3 a	3 b
Length [Å]	Fe1-Fe2	2.5584(3)	2.5920(4)	2.6046(3)
	Fe1-P1	2.1516(5)	2.1409(5)	2.1501(5)
	Fe1-P2	2.1599(5)	2.1558(6)	2.1566(5)
	Fe2-P3	2.1673(5)	2.1453(5)	2.1547(5)
	Fe2-P4		2.1630(6)	2.1628(5)
Angles [°]	P1-Fe1-P2	99.61(2)	101.08(2)	100.90(2)
	P3-Fe2-P4		98.66(2)	96.11(2)
	P1-Fe1-S1	106.09(2)	99.14(2)	101.53(2)
	P2-Fe1-S1	154.30(2)	159.73(2)	157.53(2)
	P4-Fe2-S2		157.58(2)	158.74(2)
	P3-Fe2-C2	96.73(6)		
	P3-Fe2-C3	95.27(7)		
	C3-Fe2-S1	161.07(7)		
	S1-Fe–$S2_{av}$	84.04	83.92	83.05

Table 2. IR (CH_2Cl_2; cm^{-1}) of complexes **1–3**.

Compounds	$\bar{\nu}$ (CO)	$\bar{\nu}$ $(CO)_{average}$	$\Delta\bar{\nu}$ $(CO)_{shift/parent}$
$[Fe_2(CO)_6(\mu\text{-pdt})]$ (**1 a**)[14]	2073(s), 2033(s), 1998(s), 1988(s)	2023	–
$[Fe_2(CO)_3\{P(OMe)_3\}_3(\mu\text{-pdt})]$ (**2 a**)	1979(s), 1925(s), 1907 (sh)	1937	86
$[Fe_2(CO)_2\{P(OMe)_3\}_4(\mu\text{-pdt})]$ (**3 a**)	1918(s), 1895 (s)	1907	116
$Fe_2(CO)_6(\mu\text{-}adt^{iPr})]$ (**1 b**)[15]	2072(m), 2035(s), 1995(s)	2034	–
$[Fe_2(CO)_3\{P(OMe)_3\}_3(\mu\text{-}adt^{i-Pr})]$ (**2 b**)	1976(m), 1922(s), 1907(sh)	1935	99
$[Fe_2(CO)_2\{P(OMe)_3\}_4(\mu\text{-}adt^{i-Pr})]$ (**3 b**)	1915(s), 1893 (s)	1904	130
$[Fe_2(CO)_6(\mu\text{-}adt^{Bn})]$ (**1 c**)[16]	2073(m), 2035(s), 1997(s)	2035	–
$[Fe_2(CO)_3\{P(OMe)_3\}_3(\mu\text{-}adt^{Bn})]$ (**2 c**)	1976(s), 1922(s), 1907 (sh)	1935	100
$[Fe_2(CO)_2\{P(OMe)_3\}_4(\mu\text{-}adt^{Bn})$ (**3 c**)	1915(s), 1893 (s)	1904	131

Research Article
doi.org/10.1002/ejic.202200133

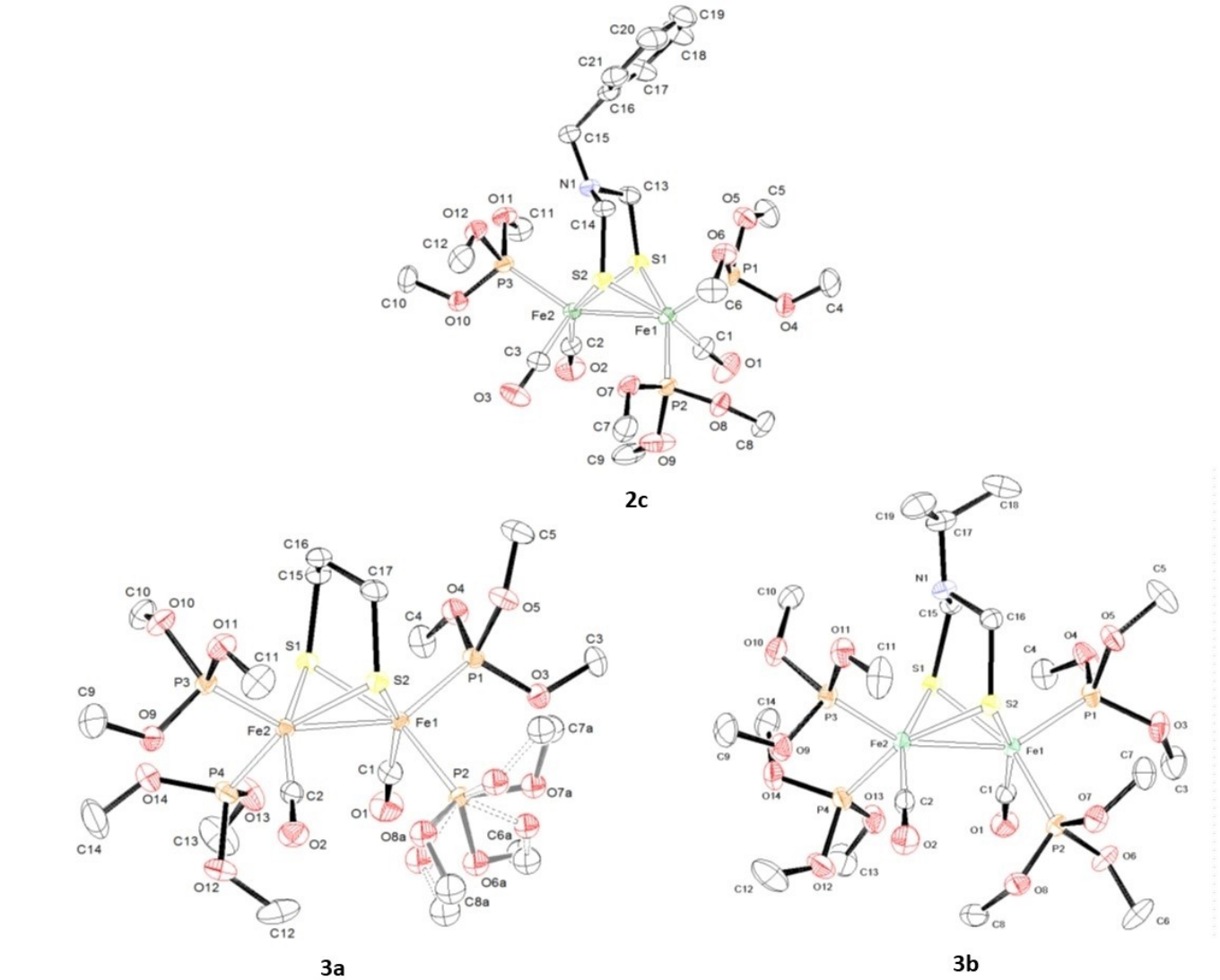

Figure 1. Ortep view (ellipsoids at 30% of probability level) of **2c**, **3a**–**b**.

The IR spectra display typical patterns of two bands in the carbonyl region for the tetra-substituted compounds,[12c] and of three bands for the related tri-substituted ones. A shift of the $\bar{\nu}$(CO) bands towards lower wavenumbers compared to those of the parent complex is consistent with a better electron-donor character of the phosphite ligand than that of the carbonyl (Table 2). As expected, the $\bar{\nu}$(CO) patterns of the tri-substituted compounds **2a**–**c** are similar, which is consistent with a similar molecular structure in solution. Likewise, IR observations in the carbonyl region for **3a**–**c** suggest a similar geometry for these tetra-substituted complexes.

^{1}H NMR spectra of tri- and tetra-substituted complexes, recorded in $CDCl_3$ at 25 °C, display the expected set of resonances for the various group, $P(OMe)_3$ and dithiolate (Experimental part). Their ^{31}P-{^{1}H} NMR spectra show broad signals, *ca* 170–190 ppm, for the phosphite ligands, that is typical of operative fluxional behaviours of such compounds in solution.[3] For this reason, variable temperature ^{31}P-{^{1}H} NMR (CD_2Cl_2) experiments were performed and revealed the temperature dependence of the line shapes of these complexes when the temperature decreases. Observations made with complexes **2b** and **3b** exemplify nicely general behaviours of tri- and tetra-substituted species in this series (Figures S1, S2) that are in agreement with previous reports.[3f,8a,12c,17] When the temperature decreases, the broad signal observed at 25 °C for **3b** splits into two large resonances at *ca* 0 °C (Figure S1a). Then, each of these resonances splits again independently into two signals, at different coalescence temperatures (*ca* −55 °C and −85 °C). At −90 °C four resonances are detected. These observations are compatible with the fluxionality expected for a transoïd basal-apical isomer. When temperature decreases, the higher energy process related to the exchange of phosphorus atoms in basal-apical position is frozen (Scheme 2a). Then at lower temperature, the slow-down of the "wiper" motion of the bridge (non-rigidity of the metallacycle $\{FeS_2C_3\}$) allows to differentiate each phosphite ligand. It is worth noting that in the case of **3a**, only

Research Article
doi.org/10.1002/ejic.202200133

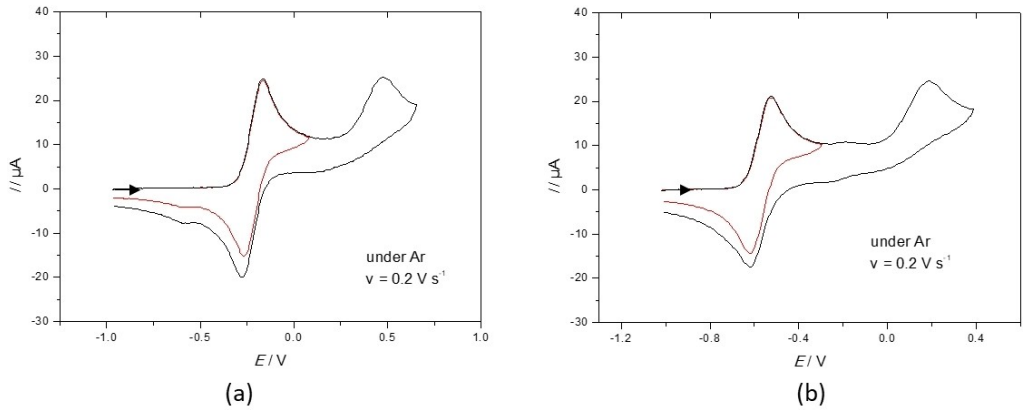

Figure 2. Cyclic voltammetry of $[Fe_2(CO)_{6-x}(P(OMe)_3)_x(\mu\text{-pdt})]$ **(a)** (x = 3, (**2a**) (1.26 mM); **(b)** (x = 4) (**3a**) (1.23 mM) in CH_2Cl_2-$[NBu_4][PF_6]$ 0.2 M under Ar at 0.2 V s^{-1}.

two peaks are observed at −90 °C, showing thus the higher flexibility of pdt bridge compared to that of the azadithiolate (Figure S1b). Tri-substituted derivatives, such as **2b**, were characterized in their $^{31}P\text{-}\{^1H\}$ NMR spectra, recorded at 25 °C in CD_2Cl_2, by a singlet, at *ca* 180 ppm, assigned to the $P(OMe)_3$ coordinated at the monosubstituted iron centre (Figure S2). This signal overlaps a wide resonance attributed to the two other $P(OMe)_3$. When the temperature decreases this last signal splits into two peaks suggesting that the basal-apical exchange between phosphite is stopped (Scheme 2b). Observations of additional weak peaks at −80 °C could be due to isomers with a different orientation of the bridge-head group of the dithiolate or a apical→basal motion of the $P(OMe)_3$ borne by the monosubstituted iron atom (Scheme 2c).[18]

Preliminary investigations of the protonation of **2a** and **3a** were performed. **2a** and **3a** were reacted in CH_2Cl_2 with HBF_4. IR monitoring in the $\bar{\nu}$(CO) region, show the appearance of two strong bands at 2050 and 1994 cm^{-1} and one intense band at 1978 cm^{-1} for **2a** and **3a**, respectively (Figure S3). These wavenumber shifts suggest a protonation at the diiron site.[17b] The formation of hydride species was confirmed by observation in ^1H NMR spectra of multiplets between −13 and −17 ppm, showing also that isomerization processes are operative upon protonation.

The electrochemical properties of complexes $[Fe_2(CO)_{6-x}(P(OMe)_3)_x(\mu\text{-pdt})]$ (x = 3) (**2a**) and (x = 4) (**3a**) were preliminary examined in CH_2Cl_2-$[NBu_4][PF_6]$ 0.2 M by cyclic voltammetry (CV) under inert atmosphere (argon) on a vitreous carbon electrode. Potentials are given versus the couple (Fc^+/Fc). The cyclic voltammograms show that **2a** has a reversible monoelectronic oxidation at $E_{1/2}^{ox1} = -0.22$ V, with a ratio ($i_p^{c,\,ox1}/i_p^{a,\,ox1}$) close to 1 (Figure 2a, Figure S4). A second oxidation at $E_p^{ox2} = 0.47$ V, assigned to the oxidation of the cation since the ratio ip^{ox2}/ ip^{ox1} is constant whatever the scan rate, is irreversible which suggests that an EC process is operative. The cation $\mathbf{2a}^+$ is, apparently, regenerated in this process since the intensity of the cathodic peak of the first oxidation is similar to that obtained when the scan is immediately reversed after the first oxidation. The substitution of a fourth CO by $P(OMe)_3$ shifts, as expected, potentials of **3a** at more negative (or less positive) potentials than those observed for **2a**: $E_{1/2}^{ox1} = -0.57$ V, $E_p^{ox2} = 0.19$ V (Figure 2b). The i_p^{ox2}/i_p^{ox1} ratio is constant at different scan rates indicating that the second irreversible oxidation corresponds to that of the cation and, as for **2a**, it occurs according to an EC mechanism causing the regeneration of the monocation $\mathbf{3a}^+$ detected on the reverse scan.

Upon successive additions of MeCN to the solution of **2a**, the increase of i_p^{ox1} with a shift of the oxidation potential, the loss of reversibility and the appearance of a new peak on the reverse scan suggest the formation of an adduct that oxidizes at a less positive potential than **2a** (Figure 3). The scan rate dependence of the current function determined in the presence of ca 1000 equivalents of acetonitrile confirms an ECE process. This is consistent with the fact that in MeCN, the oxidation of **2a** involves two electrons, which is determined by comparison of the current functions of **2a** with that of the complex $[Fe_2(CO)_4(\kappa^2\text{-}I_{Me}\text{-}CH_2\text{-}I_{Me})(\mu\text{-pdt})]$ (I_{Me} = 1-methylimidazol-2-ylidene) which has a one-electron oxidation,[19] (Figure S5). It is worth noting that the chemical reaction C (formation of MeCN coordinated species) is fast since two electrons are still involved at high scan rates.

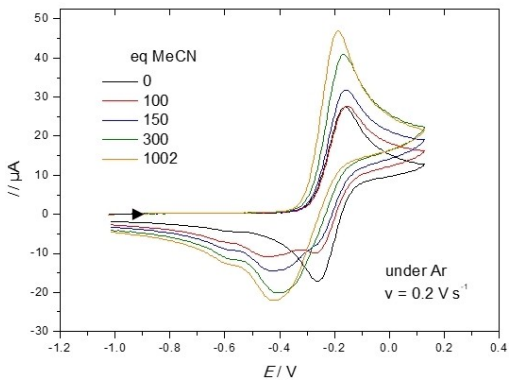

Figure 3. Cyclic voltammetry of $[Fe_2(CO)_3(P(OMe)_3)_3(\mu\text{-pdt})]$ (**2a**) (1.29 mM) in the presence of MeCN in CH_2Cl_2-$[NBu_4][PF_6]$ 0.2 M under Ar at 0.2 V s^{-1}.

Research Article
doi.org/10.1002/ejic.202200133

Upon addition of methanesulfonic acid, the oxidation peak of **2a** and **3a** decreases while a reduction peak appears at −1.64 V and −1.89 V with a shoulder at −1.81 V in the CV of **2a** and **3a**, respectively, and are thus assigned to cationic hydride species (Figures S6–S8). IR spectra of the resulting solutions were similar to those obtained upon protonation of **2a** and **3a** with HBF_4 in CH_2Cl_2 (Figure S3). In the case of **3a**, no catalysis is observed at this reduction potential. An increase of the current arises only at a more negative potential, suggesting that a catalytic event takes place in these experimental recording conditions.

Conclusion

The results described in this preliminary study show that the formation of relatively stable tri- and tetra-substituted derivatives of [$Fe_2(CO)_6$(μ-dithiolate)] using $P(OMe)_3$ ligand is attainable. Such new systems obtained with monodentate ligands, as phosphane, remain surprisingly scarce despite the fact that they could be useful electronically and sterically controlled platforms for considering further reactivity at a diiron site. Preliminary results show that such tri- and tetra-substituted derivatives can be protonated, affording thus hydride species that could be efficient for activating various small substrates. Furthermore, electrochemical studies show that they can be oxidized at accessible potentials under 0 V that should allow their oxidation by common oxidant reagents such as ferrocenium. Moreover, in MeCN, CV recordings suggest strongly that MeCN substrate is incorporated into the coordination sphere of iron atoms, showing thus the possibility to modify and to control sequentially the coordination sphere around the dinuclear site for having highly reactive species as well as the possibility to activate small molecules through oxidative processes. Extension of this work, by varying phosphane/dithiolate groups, and studies in more details of proton transfer, and oxidation in the presence of substrates, are now considered.

Experimental Section

General procedures

All the experiments were carried out under an inert atmosphere, using Schlenk techniques for the syntheses. Solvents were deoxygenated and dried according to standard procedures. Literature methods were used for the preparation of the starting materials, [$Fe_2(CO)_6$(μ-pdt)] (**1a**),[14] [$Fe_2(CO)_6$(μ-adt^{iPr})] (**1b**),[15] and [$Fe_2(CO)_6$(μ-adt^{Bn})] (**1c**);[16] all other reagents were purchased from commercial sources and used as received. IR spectra were recorded in CH_2Cl_2 solutions with a Perkin-Elmer spectrometer. NMR spectra (^{1}H, ^{31}P-{^{1}H}) were recorded either at room temperature in $CDCl_3$ or CD_2Cl_2 solutions with a Bruker AMX 400 or AC 300 spectrometer ('Service général des plateformes, Université de Bretagne Occidentale, Brest) and were referenced to $SiMe_4$ (^{1}H) and H_3PO_4 (^{31}P). VT-NMR experiments were performed with a Bruker DRX 500 spectrometer. Chemical analyses were made by the "Service de Microanalyse du CNRS", Gif/Yvette (France). Single-crystal X-ray diffraction data were collected at 170 K on an Oxford Diffraction X-Calibur-2 CCD diffractometer, equipped with a jet cooler device and a graphite-monochromated Mo–Kα radiation (λ = 0.71073). Electrochemical measurements were conducted using a PG-STAT 128 N Autolab driven by the GPES software. All the electrochemical studies were carried out in a conventional three-electrode cell under an inert atmosphere (argon). The preparation and the purification of the supporting electrolyte [NBu_4][PF_6] were as described previously.[20] The working electrode was a vitreous carbon disk of 0.3 cm in diameter, polished with alumina prior to use. A platinum wire was used as counter electrode. The reference electrode was an $Ag|Ag^+$ electrode, however, all the potentials (text, tables, and figures) are quoted against the (Fc^+/Fc) couple; ferrocene was added as an internal standard at the end of the experiments.

Synthesis of [$Fe_2(CO)_{6-x}${P(OMe)$_3$}$_x$(μ-pdt)] (x = 3 (2a), 4 (3a))

To a THF (100 mL) solution of propane dithiolate hexacarbonyl derivative [$Fe_2(CO)_6$(μ-pdt)] (**1a**) (0.5 g, 1.3 mmol), 10 equiv. of $P(OMe)_3$ (1.513 mL, 13 mmol) were added. The mixture was photolyzed under nitrogen with a UV lamp, dipping in the solution, until the starting material **1a** totally disappeared (~1 hr) as monitored by IR. After evaporation of the solvent, the residue was chromatographed on a silica gel column. Light yellow and orange bands were eluted with a dichloromethane-hexane (40:60) mixture giving, respectively, the known mono-and di-substituted derivatives[11c] in very small quantities. A third red band collected with dichloromethane gave compound **2a**. Removal of volatiles afforded a red residue that was washed with n-pentane at low temperature, to get a red powder **2a** in moderate yields (27%). Elution with a dichloromethane-THF (95:5) mixture led to a fourth dark red fraction that gave, after evaporation, compound **3a** in 16% yield, as a dark red powder. Crystals suitable for an X-ray analysis were grown from a n-pentane solution of **3a**, at room temperature.

2a: % Calcd. For $C_{15}H_{33}Fe_2O_{12}P_3S_2$: C, 26.71; H, 4.90. Found: C, 27.43; H, 4.71%. IR (CH_2Cl_2; cm^{-1}): $\bar{\nu}$ (CO) 1979(s), 1925(s), 1907(sh). ^{1}H NMR ($CDCl_3$; 298°K; ppm): δ 3.80 (d, $^3J_{PH}$ = 11.4 Hz, 9H, $P(OMe)_3$), 3.73 (d, $^3J_{PH}$ = 10.4 Hz, 18H, $P(OMe)_3$), 1.88 (m, 4H, CH_2), 1.70 (m, 1H, CH_2), 1.49 (m, 1H, CH_2). ^{1}H NMR (CD_2Cl_2; 298 K; ppm): δ 3.76 (d, $^3J_{PH}$ = 11.5 Hz, 9H, $P(OMe)_3$), 3.71 (d, $^3J_{PH}$ = 10.5 Hz, 18H, $P(OMe)_3$), 1.86 (m, 4H, CH_2), 1.70 (m, 1H, CH_2), 1.46 (m, 1H, CH_2). ^{31}P-{^{1}H} NMR ($CDCl_3$; 298 K; ppm): δ 182.6 (s, overlapping a broad signal).

3a: % Calcd. For $C_{17}H_{42}Fe_2O_{14}P_4S_2$: C, 26.49; H, 5.45. Found: C, 27.36; H, 4.86%. IR (CH_2Cl_2; cm^{-1}): $\bar{\nu}$ (CO) 1918 (s), 1895 (s). ^{1}H NMR ($CDCl_3$; 298 K; ppm): δ 3.73 (m, 36H, $P(OMe)_3$), 1.90 (m, 4H, CH_2), 1.64 (m, 2H, CH_2). ^{31}P-{^{1}H} NMR (CD_2Cl_2): 179.9 (s, br).

Synthesis of [$Fe_2(CO)_{6-x}${P(OMe)$_3$}$_x$(μ-adt^{i-Pr})](x = 3 (2b), 4(3b))

In a similar way, to a solution of 0.65 g of [$Fe_2(CO)_6$(μ-adt^{i-Pr})] (**1b**) (1.515 mmol) were added 10 equiv. of $P(OMe)_3$ (1.79 mL, ~15 mmol), in 100 mL of THF. The mixture was photolyzed with a UV lamp, dipping in solution, until compound **1b** disappeared (~1 hr). After evaporation of the solvent, the residue was purified by chromatography on silica gel. Complexes **2b** (24% yield) and **3b** (14% yield) were separated from minor side-products by elution with CH_2Cl_2/THF (98:2, and 90:10) mixtures. Single crystals of **3b** were grown from n-pentane solution at −30 °C.

2b: IR (CH_2Cl_2; cm^{-1}): $\bar{\nu}$ (CO) 1976 (s), 1922 (s), 1907 (sh). ^{1}H NMR ($CDCl_3$; 298 K; ppm): δ 3.74 (d, $^3J_{PH}$ = 11.6 Hz, 9H, $P(OMe)_3$), 3.70 (d, $^3J_{PH}$ = 10.4 Hz, 18H, $P(OMe)_3$), 2.95 (d, $^2J_{HH}$ = 9.4 Hz, 2H, CH_2), 2.72 (d, $^2J_{HH}$ = 9.4 Hz, 2H, CH_2), 2.49 (m, 1H, C*H*(CH_3)$_2$), 0.82 (d, $^3J_{HH}$ = 6.4 Hz, 6H, HC(*CH_3*)$_2$). ^{31}P-{^{1}H} NMR (CD_2Cl_2; 298 K; ppm): δ 182.6 (s, overlapping a broad signal)

3 b: IR (CH_2Cl_2; cm^{-1}): $\bar{\nu}$ (CO) 1915 (s), 1893 (s). ^1H NMR ($CDCl_3$; 298 K; ppm): δ 3.69 (m, 36H, $P(OMe)_3$), 2.85(s, 4H, CH_2), 2.46 (sept, ^3J = 6.8 Hz, 1H, $CH(CH_3)_2$), 0.82 (d, $^3J_{HH}$ = 6.8 Hz, 6H, $HC(CH_3)_2$). ^{31}P-{^1H} NMR (CD_2Cl_2; 298 K; ppm): δ 181.0 (br).

Synthesis of $[Fe_2(CO)_{6-x}\{P(OMe)_3\}_x(\mu\text{-}adt^{Bn})]$ (x = 3 (2 c), 4(3 c)).

Similarly, the reaction of $[Fe_2(CO)_6(\mu\text{-}adt^{Bn})]$ (**1 c**) (0.300 g, 0.628 mmol) with an excess of $P(OMe)_3$ (10 equiv, 0.787 mL) gave rise to two new products, after 4 hr of photolysis in THF (100 mL). The solvent was removed, and the residue chromatographed on silica gel. Complexes **2 c** and **3 c** were separated from few minor side-products by elution with CH_2Cl_2/THF (99 : 1, and 98 : 2) mixtures. These two compounds were, after works, obtained, each of them in low yields (~10%), as dark red powders from the collected bands after removal of solvents, and washing with n-pentane. Single crystals of **2 c** were obtained from a cold solution of n-pentane.

2 c: IR (CH_2Cl_2; cm^{-1}): $\bar{\nu}$ (CO) 1976 (s), 1922 (s), 1907 (sh). ^1H NMR ($CDCl_3$; 298 K; ppm): δ 7.18 (m, 5H, C_6H_5), 3.73 (d, $^3J_{PH}$ = 12.0 Hz, 9H, $P(OMe)_3$), 3.66 (d, $^3J_{PH}$ = 10.0 Hz, 18H, $P(OMe)_3$), 3.42 (s, 2H, CH_2(Bn)), 2.95 (d, J_{HH} = 9.2 Hz, 2H, CH_2), 2.71 (br, 2H, CH_2). ^{31}P-{^1H} NMR (CD_2Cl_2; 298 K; ppm): δ 181.8 (s), 180.5 (br).

3 c: IR (CH_2Cl_2; cm^{-1}): $\bar{\nu}$ (CO) 1915 (s), 1893 (s). ^1H NMR ($CDCl_3$; 298 K; ppm): δ 7.23 (d, J_{HH} = 7.2 Hz, 2H, C_6H_5), 7.18 (d, J_{HH} = 7.6 Hz, 1H, C_6H_5), 7.08 (d, J_{HH} = 6.8 Hz, 2H, C_6H_5), 3.67 (m, 36H, $P(OMe)_3$), 3.45 (s, 2H, CH_2(Bn)), 2.87 (s, 4H, CH_2). ^{31}P-{^1H} NMR (CD_2Cl_2; 298 K; ppm): 180.0 (br)

Crystallography

The structures of **2 c** and **3 a**–**b** were solved by direct methods and refined by full-matrix least-squares on [F^2].[21] Complete crystal data and parameters for data collection and refinement are listed in Table S1 (SI).

Deposition Numbers 2153355 (for **3 a**), 2153357 (for **3 b**), and 2153358 (for **2 c**) contain the supplementary crystallographic data for this paper. These data are provided free of charge by the joint Cambridge Crystallographic Data Centre and Fachinformationszentrum Karlsruhe Access Structures service www.ccdc.cam.ac.uk/structures.

Acknowledgements

CNRS (Centre National de la Recherche Scientifique) and the Université de Bretagne Occidentale (Brest) are acknowledged for financial support. Stay and travel of F. Realini were funded by ERASMUS + exchange program between Universities of Brest and Milano-Biccoca. NMR recordings were performed at the 'Service général des plateformes, Brest' (SGPLAT). We are grateful to Dr. F. Michaud for the crystallographic measurements of complexes and to the SGPLAT for VT-NMR recordings on Bruker DRX 500 spectrometer.

Conflict of Interest

The authors declare no conflict of interest.

Data Availability Statement

The data that support the findings of this study are available from the corresponding author upon reasonable request.

Keywords: Bioinspired models · Hydrides · Hydrogenases · Iron · Phosphine ligands · Thiolate ligands

[1] a) J. W. Peters, W. N. Lanzilotta, B. J. Lemon, L. C. Seefeldt, *Science* **1998**, *282*, 1853–1858; b) Y. Nicolet, C. Piras, P. Legrand, C. E. Hatchikian, J. C. Fontecilla-Camps, *Structure* **1999**, *7*, 13–23.

[2] a) W. Lubitz, H. Ogata, O. Rüdiger, E. Reijerse, *Chem. Rev.* **2014**, *114*, 4081–4148; b) J. A. Birell, P. Rodriguez-Macia, E. J. Reijerse, M. A. Martini, W. Lubitz, *Coord. Chem. Rev.* **2021**, *449*, 214191.

[3] a) C. Tard, C. J. Pickett, *Chem. Rev.* **2009**, *109*, 2245–2274; b) U.-P. Apfel, F. Y. Pétillon, P. Schollhammer, J. Talarmin, W. Weigand, *'[FeFe] Hydrogenase Models: An Overview' in 'Bioinspired Catalysis: Metal-Sulfur Clusters'* (Ed.: W. Weigand, P. Schollhammer), Wiley-VCH, **2014** chapter 4, pp 79–105; c) D. Schilter, J. M. Camara, M. T. Huynh, S. Hammes-Schiffer, T. B. Rauchfuss, *Chem. Rev.* **2016**, 116, 8693–8749; d) C. Elleouet, F. Y. Pétillon, P. Schollhammer, *'[FeFe]-hydrogenases Models' in 'Advances in bioorganometallic chemistry'*, Ed. T. Hirao, T. Moriuchi, Elsevier, **2019**, chapter 17, pp 347–359; e) T. R. Simmons, G. Berggren, M. Bacchi, M. Fontecave, V. Artero, *Coord. Chem. Rev.* **2014**, *270–271*, 127–150; f) J.-F. Capon, F. Gloaguen, F. Y. Pétillon, P. Schollhammer, J. Talarmin, *Eur. J. Inorg. Chem.* **2008**, 4671–4681; g) J. A. Wright, C. J. Pickett in *Bioinspired Catalysis: Metal-Sulfur Clusters* (Ed.: W. Weigand, P. Schollhammer), Wiley-VCH, **2014**, chapter 7, pp 161–198; h) C. Greco, L. De Gioia, in *Bioinspired Catalysis: Metal-Sulfur Clusters* (Ed.: W. Weigand, P. Schollhammer), Wiley-VCH, **2014**, chapter 6, pp 137–160; i) A. Aster, S. Wang, M. Mirmohades, C. Esmieu, G. Berggren, L. Hammarström, R. Lomoth, *Chem. Sci.* **2019**, *10*, 5582–5588; j) C. Elleouet, F. Y. Pétillon, P. Schollhammer, in *Non-Noble Metal Catalysis – Molecular Approaches and Reactions: Non-noble metal-based molecular catalysts for protons reduction* (Ed.: R. J. M. Klein Gebbink, M. E. Moret), Wiley-VCH, **2019**, chapter 19, pp 489–527; k) J.-F. Capon, F. Gloaguen, F. Y. Pétillon, P. Schollhammer, J. Talarmin, *Coord. Chem. Rev.* **2009**, *253*, 1476–1494; l) J. T. Kleinhaus, F. Wittkamp, S. Yadav, D. Siegmund, U.-P. Apfel, *Chem. Soc. Rev.* **2021**, *50*, 1668–1784.

[4] a) J. M. Camara, T. B. Rauchfuss, *Nat. Chem.* **2012**, *4*, 26–30; b) J. C. Lansing, J. M. Camara, D. E. Gray, T. B. Rauchfuss, *Organometallics* **2014**, *33*, 5897–5906; c) T. B. Rauchfuss, *Acc. Chem. Res.* **2015**, *48*, 2107–2116.

[5] a) M. Watanabe, Y. Honda, H. Hagiwara, T. Ishihara, *J. Photochem. Photobiol. C* **2017**, *33*, 1–26; b) F. Möller, S. Piontek, R. G. Miller, U.-P. Apfel, *Chem. Eur. J.* **2018**, *24*, 1471–1493; c) S. Gao, W. Fan, Y. Liu, Q. Duan, *Int. J. Hydrogen Energy* **2020**, *45*, 4305–4327; d) L.-Z. Wu, B. Chen, Z.-J. Li, C.-H. Tung, *Acc. Chem. Res.* **2014**, *47*, 2177–2185; e) M. Wang, K. Han, S. Zhang, L. Sun, *Coord. Chem. Rev.* **2015**, *287*, 1–14.

[6] a) M. Haumann, S. T. Stripp, *Acc. Chem. Res.* **2018**, *51*,1755–1763; b) H. Land, M. Senger, G. Berggren, S. T. Stripp, *ACS Catal.* **2020**, *10*, 7069–7086; c) F. Wittkamp, M. Senger, S. T. Stripp, U.-P. Apfel, *Chem. Commun.* **2018**, *54*, 5934–5942.

[7] a) J. H. Artz, O. A. Zadvornyy, D. W. Mulder, S. M. Keable, A. E. Cohen, M. W. Ratzloff, S. G. Williams, B. Ginovska, N. Kumar, J. Song, S. E. McPhillips, C. M. Davidson, A. Y. Lyubimov, N. Pence, G. J. Schut, A. K. Jones, S. M. Soltis, M. W. W. Adams, S. Raugei, P. W. King, J. W. Peters, *J. Am. Chem. Soc.* **2020**, *142*, 1227–1235; b) J. A. Birell, V. Pelmenschikov, N. Mishra, H. Wang, Y. Yoda, K. Tamasaku, T. B. Rauchfuss, S. P. Cramer, W. Lubitz, S. DeBeer, *J. Am. Chem. Soc.* **2020**, *142*, 222–232.

[8] a) A. Hobballah, S. Lounissi, R. Motei, C. Elleouet, F. Y. Pétillon, P. Schollhammer, *Eur. J. Inorg. Chem.* **2021**, 205–216; b) A. Hobballah, F. Arrigoni, C. Elleouet, C. Greco, M. Laurans, F. Y. Pétillon, P. Schollhammer, *Inorg. Chem. Front.* **2021**, *8*, 3659–3674; c) L. Almazahreh, F. Arrigoni, H. Abul-Futouh, M. El-khateeb, H. Görls, C. Elleouet, P. Schollhammer, L. De Gioia, M. Rudolph, G. Zampella, W. Weigand, *ACS Catal.* **2021**, *11*, 7080–7098; d) F. Arrigoni, C. Elleouet, L. De Gioia, A. Mele, F. Y. Pétillon, P. Schollhammer, G. Zampella, *Chem. Eur. J.* **2020**, *26*, 17536–17545.

[9] G. Filippi, F. Arrigoni, L. Bertini, L. De Gioia, G. Zampella, *Inorg. Chem.* **2015**, *54*, 9529–9542.

[10] a) R. B. King, T. E. Bitterwolf, *Coord. Chem. Rev.* **2000**, *206–207*, 563–579; b) M. Y. Daresbourg, E. J. Lyon, J. J. Smee, *Coord. Chem. Rev.* **2000**, *206–207*, 522–561; c) Y. Li, T. B. Rauchfuss *Chem. Rev.* **2016**, *116*, 7043–7077; d) for a recent example: S. Ghosh, A. Rahaman, G. Orton, G. Gregori, M. Bernat, U. Kulsume, N. Hollingsworth, K. B. Holt, S. E. Kabir, G. Hogarth, *Eur. J. Inorg. Chem.* **2019**, 4505–4515.

[11] See for selected examples : a) J. A. De Beer, R. J. Haines, *J. Organomet. Chem.* **1972**, *37*, 173–181; b) P. Li, M. Wang, C. He, G. Li, X. Liu, C. Chen, B. Äkermark, L. Sun, *Eur. J. Inorg. Chem.* **2005**, 2506–2513; c) D. Morvan, J.-F. Capon, F. Gloaguen, P. Schollhammer, J. Talarmin, *Eur. J. Inorg. Chem.* **2007**, 5062–5068; d) H.-M. Lin, C. Mu, A. Li, X.-F. Liu, Y.-L. Li, Z.-Q. Jiang, H.-K. Wu, *Transition Met. Chem.* **2019**, *44*, 491–498 ; e) L. R. Almazahreh, W. Imhof, J. Talarmin, P. Schollhammer, H. Görls, M. El-khateeb, W. Weigand, *Dalton Trans.* **2015**, *44*, 7177–7189 ; f) H. Abul-Futouh, L. R. Almazahreh, S. J. Abaalkhail, H. Görls, S. T. Stripp, W. Weigand, *New J. Chem.* **2021**, *45*, 36–44; g) A. Q. Daraosheh, M. K. Harb, J. Windhager, H. Görls, M. El-khateeb, W. Weigand, *Organometallics* **2009**, *28*, 6275–6280; h) H. Abul-Futouh, H. Görls, W. Weigand, *Z. Anorg. Allg. Chem.* **2017**, *643*, 1615–1620; i) J. H. Blank, S. Moncho, A. M. Lunsford, E. N. Brothers, M. Y. Darensbourg, A. A. Bengali, *Chem. Eur. J.* **2016**, *22*, 12752–12760; j) P. C. Ellgen, J. N. Gerlach, *Inorg. Chem.* **1973**, *12*, 2526–2532; k) S. Aime, G. Gervasio, R. Rossetti, P. L. Stanghellini, *Inorg. Chim. Acta* **1980**, *40*, 131–140; l) N. B. Makouf, H. B. Mousser, A. Darchen, A. Mousser, *J. Organomet. Chem.* **2018**, *866*, 35–42; m) F. Gloaguen, D. Morvan, J.-F Capon, P. Schollhammer, J. Talarmin, *J. Organomet. Chem.* **2007**, *603*, 15–20; n) C. Orain, F. Quentel, F. Gloaguen, *ChemSusChem* **2014**, *7*, 638–643; o) F. Quentel, G. Passard, F. Gloaguen, *Chem. Eur. J.* **2012**, *18*, 13473–13479; p) A. Darchen, H. Mousser, H. Patin, *J. Chem. Soc. Chem. Commun.* **1988**, 968–970.

[12] a) J. I. van der Vlugt, T. B. Rauchfuss, C. M. Whaley, S. R. Wilson, *J. Am. Chem. Soc.* **2005**, *127*, 16012–16013; b) M. G. Galinato, C. M. Waley, D. Roberts, P. Wang, N. Lehnert, *Eur. J. Inorg. Chem.* **2011**, 1147–1154; c) R. Zaffaroni, T. B. Rauchfuss, D. L. Gray, L. De Gioia, G. Zampella, *J. Am. Chem. Soc.* **2012**, *134*, 19260–19269; d) Q. Li, N. Lalaoui, T. J. Woods, T. B. Rauchfuss, F. Arrigoni, G. Zampella, *Inorg. Chem.* **2018**, *57*, 4409–4418.

[13] M. L. Singleton, R. M. Jenkins, C. L. Klemashevich, M. Y. Darensbourg, *C. R. Chim.* **2008**, *11*, 861–874.

[14] a) E. J. Lyon, I. P. Georgakaki, J. H. Reibenspies, M. Y. Darensbourg, *Angew. Chem. Int. Ed.* **1999**, *38*, 3178–3180; *Angew. Chem.* **1999**, *111*, 3373–3376; b) A. Winter, L. Zsolnai, G. Huttner, *Z. Naturforsch.* **1982**, *37 b*, 1430–1436; c) C. F. Works, *J. Chem. Educ.* **2007**, *84*, 836–838.

[15] J.-F. Capon, S. Ezzaher, F. Gloaguen, F. Y. Pétillon, P. Schollhammer, J. Talarmin, T. J. Davin, J. E. Mc Grady, K. W. Muir, *New J. Chem.* **2007**, *31*, 2052–2064.

[16] S. Ezzaher, J.-F. Capon, F. Gloaguen, F. Y. Pétillon, P. Schollhammer, J. Talarmin, *Inorg. Chem.* **2007**, *46*, 9863–9872.

[17] a) A. K. Justice, G. Zampella, L. De Gioia, T. B. Rauchfuss, J. I. van der Vlugt, S. R. Wilson, *Inorg. Chem.* **2007**, *47*, 1655–1664; b) S. Ezzaher, J.-F. Capon, F. Gloaguen, N. Kervarec, F. Y. Pétillon, R. Pichon, P. Schollhammer, J. Talarmin, *C. R. Chim.* **2008**, *11*, 906–914.

[18] P.-Y. Orain, J.-F. Capon, F. Gloaguen, F. Y. Pétillon, P. Schollhammer, J. Talarmin, G. Zampella, L. De Gioia, T. Roisnel, *Inorg. Chem.* **2010**, *49*, 5003–5008.

[19] D. Morvan, J.-F. Capon, F. Gloaguen, A. Le Goff, M. Marchivie, F. Michaud, P. Schollhammer, J. Talarmin, J.-J. Yaouanc, R. Pichon, N. Kervarec, *Organometallics* **2007**, *26*, 2042–2052.

[20] F. Arrigoni, S. Mohamed Bouh, C. Elleouet, F. Y. Pétillon, P. Schollhammer, L. De Gioia, G. Zampella, *Chem. Eur. J.* **2018**, *24*, 15036–15051.

[21] Programs used: a) G. M. Sheldrick, *SHELX97*, University of Göttingen: Göttingen, Germany, **1998**; b) *Win GX-A Windows Program for Crystal Structure Analysis*, L. J. Farrugia, *J. Appl. Crystallogr.* **1999**, *32*, 837–838.

Manuscript received: February 28, 2022
Revised manuscript received: March 28, 2022
Accepted manuscript online: March 29, 2022